

University of New South Wales  
Faculty of Science  
School of Materials Science and Engineering



## **“Preliminary” PhD Thesis**

### **Biocompatible Thin Film Metallic Glasses (TFMGs)**

PhD Candidate: Scott Gleason

Supervisor: Professor Michael Ferry

## ABSTRACT

---

### General abstract structure

Problem investigated

Procedures followed

Principle results obtained

Major conclusion reached

## TABLE OF CONTENTS

Abstract .....	i
Table of Contents .....	ii
List of Figures .....	iv
1 Introduction .....	1
2 Proposal .....	1
2.1 Aims.....	1
2.1.1 TFMG Characterization .....	1
2.1.1.1 Substrates .....	1
2.1.1.2 Physical and Chemical Properties .....	1
2.1.1.3 Biocompatibility and Bioabsorption .....	1
2.1.1.4 Quality of Deposition .....	1
2.2 Methods .....	2
2.2.1 Magnetron Sputtering .....	2
2.2.1.1 Initial Sputtering Methods and Parameters.....	2
2.2.1.2 Target Preparation and Notes.....	2
2.2.1.3 Substrates Preparation and Notes.....	2
3 Literature Survey.....	3
3.1 Metallic Glasses (MGs).....	3
3.1.1 MGs Properties .....	3
3.1.2 Theory of MG Production .....	3
3.1.2.1 Solidification, Super Cooled Liquid (SCL), and Glass Transition ( $T_g$ ) .....	3
3.1.2.2 Glass Forming Ability (GFA) and Bulk Metallic Glasses (BMGs) .....	4
3.1.2.3 BMG Manufacture Methods.....	5
3.1.2.3.1 Thermoplastic Forming (TPF) Processing.....	6
3.2 Thin Films .....	7
3.2.1 Deposition.....	7
3.2.1.1 Pulsed Laser Deposition (PLD) .....	7
3.2.1.2 Sputtering Deposition .....	8
3.2.1.2.1 Direct Current (DC) Sputtering.....	8
3.2.1.2.2 Magnetron Sputtering .....	9
3.2.2 Thin Film Properties .....	10
3.2.3 Thin Film Adhesion.....	10
3.2.4 Ultrastable Metallic Glass (SMG) .....	10
3.2.4.1 SMG Production .....	10

3.2.4.1.1	Potential Production Issues .....	11
3.2.4.2	SMG Properties and Characteristics .....	11
3.2.4.2.1	Differential Scanning Calorimetry (DSC), Kinetic Stability and Enthalpy .....	11
3.2.4.2.2	The Theoretical Entropy Limit of Glasses and the Kauzmann Temperature $T_k$ .....	12
3.2.4.2.3	Glass Fragility $m$ .....	13
3.2.4.2.4	Indentation Modulus $M$ .....	15
3.3	Biomedical.....	16
3.3.1	Bioreabsorption / Corrosion .....	16
3.3.2	Anti-biotic Scaffolds .....	16
4	References .....	17
5	Appendices.....	19
5.1	Glossary.....	19

## LIST OF FIGURES

Figure 1: Schematic of specific enthalpy ( $h$ ) or specific volume ( $v$ ) as a function of temperature for a material that exhibits both glass and crystalline solid states. Note 'glass 1' has a greater $T_g$ and accordingly greater $h$ & $v$ than 'glass 2.' This higher temperature stability is the result of 'glass 1' be cooled more quickly than 'glass 2.' Modified from [4].	4
Figure 2: Schematic of critical cooling rate ( $R_c$ ) and maximum sample thickness ( $t_{max}$ ) as a function of reduced glass transition temperature ( $T_g/T_m$ ) for a number of glass forming systems. Note the $R_c$ and $t_{max}$ improve with increasing $T_g/T_m$ . Modified from [7].	5
Figure 3: Schematic TTT diagram where line (1) indicates the slowest cooling rate possible to avoid crystallisation and achieve the metallic glass state, and line (2) an elevated temperature processing window above $T_g$ where metallic glass displays excessive plastic deformation. Reproduced from [8].	6
Figure 4: Schematic of a typical PLD setup showing the incoming laser beam inclined at an approximate $45^\circ$ angle to the target, and the target and substrate parallel to each other. Adapted from [9].	7
Figure 5: Amorphous target XRD scan before (black curve) and after (red curve) PLD showing the shift from characteristic amorphous structure to crystalline. Reproduced from [12].	8
Figure 6: Schematic of a typical DC sputtering setup with an Ar working gas. The high-voltage field generates and propels $Ar^+$ ions toward the negative target of material "M." Dislodged "M" atoms are hurled in all directions with some being deposited on the positive substrate. Adapted from [13].	9
Figure 7: An integrated DSC trace for the molecular IMC glass system displaying the various values of $T_f$ obtained when varying the deposition rate (the coloured line). Note all deposited glasses have a reduced $T_f$ indicating a reduction in enthalpy compared to ordinary glass. Reproduced from [26].	12
Figure 8: Schematic of solidification/liquid glass temperature vs entropy in a typical glass forming system. The Kauzmann temperature ( $T_k$ ) represents the glass transition temperature ( $T_g$ ) of an ideal glass. The blue line is the extrapolated SCL line and the ideal path. Modified from [26].	13
Figure 9: Schematic of fragility for strong and weak glasses over the liquid range of viscosities. Note the 'ideal' strong liquid display a constant exponential slope over the full temperature range, while weaker liquids' slopes change. Reproduced from [28].	14
Figure 10: Schematic of the relationship between glass fragility ( $m$ ) and the enhanced glass transition on glass transition ( $\delta T_g/T_g$ ) for a selection of metallic, molecular, and polymer USGs. Reproduced from [1].	15

# 1 INTRODUCTION

---

Biocompatible films offer new possibilities in drug delivery and orthopaedic applications. Coating pharmaceutical scaffolds with tailored bioabsorbable films could allow for slow release of drug packages such as antibiotics, antimicrobials, and analgesics (painkillers). Films have also been shown to have significant effects on the properties of their substrates, which could allow for useful modification of orthopaedic devices like plates and fasteners. These application have the potential for great changes in wound healing and pain management.

## 2 PROPOSAL

---

### 2.1 AIMS

The aims of this thesis are to produce and investigate quality thin film metallic glasses (TFMGs) for biomedical applications. TFMGs of established bulk metallic glass (BMG) compositions, such as  $\text{Mg}_{65}\text{Zn}_{30}\text{Ca}_5$  and  $\text{Mg}_{65}\text{Cu}_{25}\text{Y}_{10}$ , will be deposited on a number of different substrates. The properties and characteristics of the films as well as their effects on the different substrates will be investigated, and the characterised films compared with their BMG counterparts.

#### 2.1.1 TFMG Characterization

The properties of the TFMGs will be investigated via characterising the films after application to different substrates, allowing standalone films as well as their effects on the substrates to be investigated.

##### 2.1.1.1 Substrates

The substrates to be investigated are:

- No substrate (base TFMG only);
- Antimicrobial or Antibiotic-Infused polycaprolactone (PCL) Scaffolds; and
- BMGs of similar composition to the TFMGs.

##### 2.1.1.2 Physical and Chemical Properties

The physical and chemical properties of the TFMGs will be characterized via a range of techniques; XRD, DSC, FIB-SEM, EPMA, ICP, etc.

##### 2.1.1.3 Biocompatibility and Bioabsorption

The biocompatibility and bioabsorption of the TFMGs will be characterized via cytotoxicity testing, PDP scans, etc.

##### 2.1.1.4 Quality of Deposition

The quality of the TFMG deposition will be ascertained via investigation of the surface finish, coating adhesion, bonding, etc.

## 2.2 METHODS

The TFMGs will be deposited onto the various substrates via physical vapour deposition (PVD) processes.

### 2.2.1 Magnetron Sputtering

Magnetron sputtering with an Ar working gas will be the preferred deposition technique, although pulse laser deposition (PLD) may be used as well (See section 3.2.1 Deposition).

#### 2.2.1.1 Initial Sputtering Methods and Parameters

The initial sputtering parameters will be based on the work of Yu, et al. [1] on ultrastable  $Zr_{65}Cu_{27.5}Al_{7.5}$  TFMGs and of Liu, et al. [2] on refining the deposition parameters for the  $Zr_{55}Cu_{30}Ni_{15}Al_{10}$  TFMGs. These will be refined via appropriate step sizes as required to suit the examined biocompatible systems.

Parameters:

- Base chamber pressure: Better than  $3 \times 10^{-4}$  Pa (ideally better than  $5 \times 10^{-5}$  Pa);
- Deposition argon pressure:  $5 \times 10^{-2} - 3.0$  Pa;
- Deposition power range: 30 – 50 W;
- Deposition Rate: To be determined via TEM, with an ideal rate of  $1.4 \text{ nm s}^{-1}$ ;
- Substrate deposition temperature:  $0.7 - 0.8 T_g$ ;

#### 2.2.1.2 Target Preparation and Notes

Targets will be crystalline alloys of  $Mg_{65}Zn_{30}Ca_5$  and  $Mg_{65}Cu_{25}Y_{10}$ . The master alloys will be produced via induction furnace and formed via traditional casting techniques. Targets will be prepared for deposition via a pre-sputter to remove contamination and oxides from their surfaces.

#### 2.2.1.3 Substrates Preparation and Notes

To produce the desired TFMGs the substrates will need to be at an elevated temperate of  $0.7 - 0.8 T_g$ . These temperatures will be achieved and controlled via a hot plate and thermocouple.

Furthermore, substrates will be prepared and procured as below:

- No substrate (base TFMG only);
  - TFMGs will be deposited onto NaCl wafer (or other water soluble) substrates;
  - NaCl wafers will be procured (not manufactured);
  - Films will later be separated from substrates via dissolving in water, or other manual removal methods;
- Antimicrobial or Antibiotic-Infused PCL Scaffolds;
  - PCL Scaffolds will be procured (not manufactured);
- BMGs of similar composition to the TFMGs;
  - BMG substrates will be produced from master alloys (see 2.2.1.2 Target Preparation and Notes) and amorphous casting techniques.

**Commented [SG1]:** Probably will be much closer to the 50 W end (Jake topped out at 55 W).  
MgCaZn has more light elements near Ar than ZrCuNiAl. Therefore expect greater deposition efficiencies and to not require as much power.  
ZrCuNiAl used 50 – 150 W, but we cannot get power that high unless we use 3 inch targets (not practical).

**Commented [SG2]:** Literature review shows there is minimal benefit to using BMG targets.

## 3 LITERATURE SURVEY

### 3.1 METALLIC GLASSES (MGs)

Metallic glasses (MGs) are alloys which exhibit an amorphous structure with no long range order. This lack of an ordered structure results in MGs possess a range of unique properties which make them distinct even from traditional crystalline alloys of similar composition.

#### 3.1.1 MGs Properties

The unique properties of MGs are largely the result of their lack of crystalline structure and grain boundaries. As these amorphous alloys have no grain boundaries, they have essentially eliminated the principal structural and chemical weaknesses in metallic systems. This serves to provide MGs with superior strength, hardness, corrosion, oxidation and wear resistance, and low coefficients of friction when compared with conventional crystalline alloys.

These amorphous MG alloys also generally display large amounts of elastic deformation, although their plastic deformation is significantly limited by their lack of structure and grain boundaries as there is no mechanisms for dislocation movement. Thus when MGs fail at high stress it tends to via brittle fracture mechanisms, although it should be emphasised MGs are far less brittle than organic glasses, owing to their non-directional metallic bonds [3]. The failure mechanisms of MGs are also highly dependent on temperature and can shift from brittle to ductile, as will be explained in the following sections.

#### 3.1.2 Theory of MG Production

The production of MGs requires metallic alloys to be solidified in such a way as to produce stable amorphous structures. This is accomplished via the high cooling rates achieved through rapid quenching from the liquid or vapour states. The physical mechanisms that make this possible are described below.

##### 3.1.2.1 Solidification, Super Cooled Liquid (SCL), and Glass Transition ( $T_g$ )

Most liquid materials when cooled to their melting temperature ( $T_m$ ) undergo a phase change into an ordered solid with a repeating crystalline structure. As this is a first-order thermodynamic phase change the entire process occurs solely at the  $T_m$  and is observed as an enthalpy ( $H$ ) and volume ( $V$ ) discontinuity. As the ordered structure is at a lower energy and generally more dense than the amorphous liquid both the  $H$  and  $V$  discontinuities are negative, with a notable exception being water where the  $V$  increases.

Despite the thermodynamic driving force liquids are generally cooled below their  $T_m$  before they begin to solidify because they require a stable nucleus to initiate the process. This solidification is described by Gibbs Free Energy Theory for homogeneous and heterogeneous nucleation. In brief, a stable nucleus initiates solidification by reaching a size where further growth requires less energy than melting, providing the driving force for the phase change. Refer to "Gibbs Free Energy" for specific details which are not covered here within.

When the liquid is cooled below its  $T_m$  without solidifying it is termed a super cooled liquid (SCL). Amorphous solids, or glasses, are formed from SCL by cooling at rates sufficient to suppress the nucleation process entirely. As the SCL is cooled its viscosity ( $\eta$ ) increases while its  $H$  and  $V$  decrease linearly with temperature at the same rate as the liquid state. As the  $\eta$  approaches about  $10^{12}$  Pa\*s the time scale for molecular rearrangement of the SCL becomes significantly longer than experimental observation and the SCL is for all practical purposes 'frozen' as a glass [4]. This transition occurs at the



glass transition temperature ( $T_g$ ) and is characterised by decrease in rate of change of  $H$  and  $V$  with temperature. Note this is not a phase change, but a rather kinetic event, meaning the material is not technically thermodynamically or kinetically stable, even though it is stable for all intents and purposes [4]. Because of this the actual  $T_g$  of a glass depends on the cooling rate (i.e. is not a fixed property like  $T_m$ ) with faster cooling rates generally resulting in higher  $T_g$ , indicating the glass is suitable for use at higher service temperatures, see Figure 1.

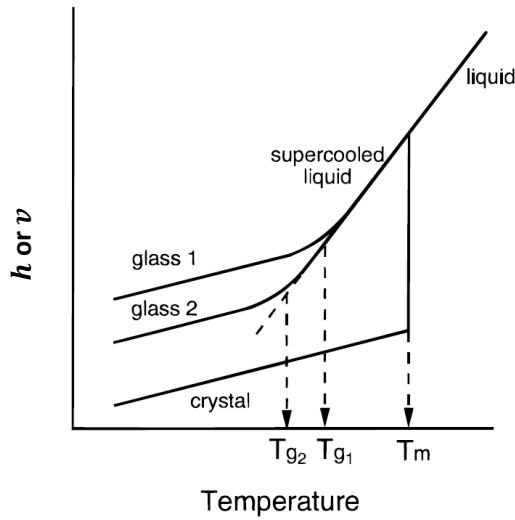


Figure 1: Schematic of specific enthalpy ( $h$ ) or specific volume ( $v$ ) as a function of temperature for a material that exhibits both glass and crystalline solid states. Note 'glass 1' has a greater  $T_g$  and accordingly greater  $h$  &  $v$  than 'glass 2.' This higher temperature stability is the result of 'glass 1' be cooled more quickly than 'glass 2.' Modified from [4].

### 3.1.2.2 Glass Forming Ability (GFA) and Bulk Metallic Glasses (BMGs)

The ease at which a material is able to form a glass is termed its glass forming ability (GFA). Organic glass' GFA is such that the material has been produced since ancient times, and polymers' GFAs are often high enough they can form glass even with very slow cooling rates. This is in contrast to metals which have GFAs so low their amorphous glass state was only discovered as recently as 1960 by Klement, et al. [5].

Much of the work on MGs has been to improve their GFAs in order to decrease their critical cooling rate ( $R_c$ ), the rate of quench required to avoid nucleation into the crystalline state [6]. From these works it has been discovered alloys with their  $T_g$  near their  $T_m$  have higher GFA [6, 7]. Meaning the GFA of an alloy increases with its reduced glass transition temperature ( $T_g/T_m$ ) [6, 7].

From these works Inoue [6] has formulated three rules for high GFA systems;

1. Multi-component systems of three or more alloy constituents;
2. Significant difference of above 12% in atomic size ratios of the three main constituents; and
3. Negative heats of mixing among the three main constituents (i.e. endothermic reaction).

Alloys that follow these rules display deep eutectics with low  $T_m$ , sluggish crystallization kinetics, and accordingly a high  $T_g/T_m$  [6, 8]. The application of these rules has helped to lower  $R_c$  sufficiently to produce alloys with maximum sample thicknesses ( $t_{max}$ ) of over 1 mm.

Amorphous alloys with their smallest dimension of at least 1 mm are formally referred to as bulk metallic glass (BMG) formers. The difference between MGs and BMGs is the later possess GFAs sufficiently high enough to allow these greater dimensions. As such alloys of BMG composition are of great interests regardless of the desired dimensions (Figure 2).

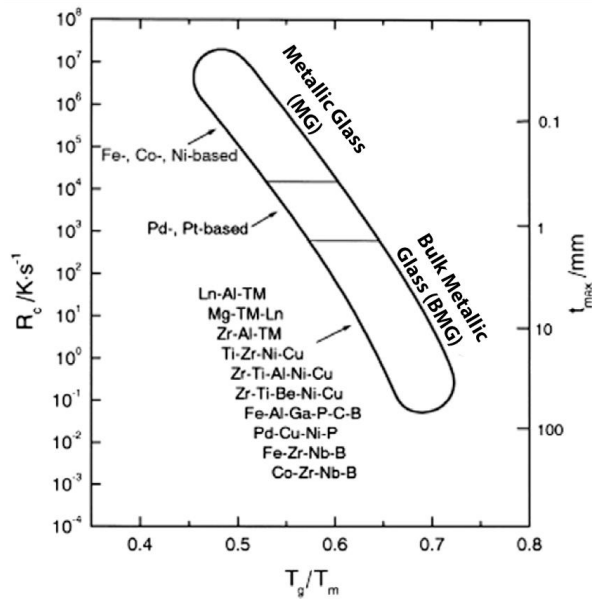


Figure 2: Schematic of critical cooling rate ( $R_c$ ) and maximum sample thickness ( $t_{max}$ ) as a function of reduced glass transition temperature ( $T_g/T_m$ ) for a number of glass forming systems. Note the  $R_c$  and  $t_{max}$  improve with increasing  $T_g/T_m$ . Modified from [7].

### 3.1.2.3 BMG Manufacture Methods

As previously mentioned, the production of MGs and BMGs requires alloys be rapidly quenched at a rate equal or better than their  $R_c$  in order to avoid crystallisation. For bulk samples this is often accomplished from the liquid state via four standard methods:

- Gravity Casting: Molten metal is poured under an air atmosphere into a copper mould to solidify.
- Injection Casting: Molten metal under an inert atmosphere is forced via pressure into a copper mould to solidify.
- Melt Spinning: Molten metal is solidified onto a water cooled copper wheel, producing ribbons of material.
- Strip Casting: Molten metal is extruded between two water cooled copper rollers, producing continuous plate.

These methods yield cooling rate sufficient for production of BMGs with simple geometries, but do not allow for complex shapes. More complex shape are accomplish through secondary processing above the  $T_g$  as described next.

### 3.1.2.3.1 Thermoplastic Forming (TPF) Processing

A unique property of amorphous metals are once formed they can be heated above their  $T_g$  into the SCL temperature range without crystallising for an appreciable amount of time. This is possible because BMGs possess sufficient thermal stability above their  $T_g$  to maintain their amorphous structure, i.e. the kinetics for crystallisation are slow [8]. At these elevated temperatures BMGs display dramatic softening as their  $\eta$  reduces to SCL values, enabling the constituent atoms to flow more freely past each other.

The introduction of this temporary plastic deformation mechanism allows BMGs to be post-processed via thermoplastic forming (TPF) techniques, similar to thermoplastic polymers. Once the elevated temperature processing is complete the newly formed BMG components can be slowly cooled below the  $T_g$  to the glassy state without initiating crystallisation. This slow cooling helps to eliminate internal stresses and allow for high dimensional accuracy in complex BMG components [8]. Note this processing is unique to BMG systems as the more rigid and limited plastic deformation mechanisms of conventional crystalline metallic systems do not support the high deformation TPF.

Figure 3 shows a TTT diagram for a generic BMG. This image shows the minimum  $R_c$  quench required to completely miss crystallisation nucleation when forming the BMG as line (1). Line (2) then displays an elevated temperature processing window available for post-processing of the formed BMG. Note with the processing window stays below the crystallisation zone and the slow cooling rate once this post processing is complete.

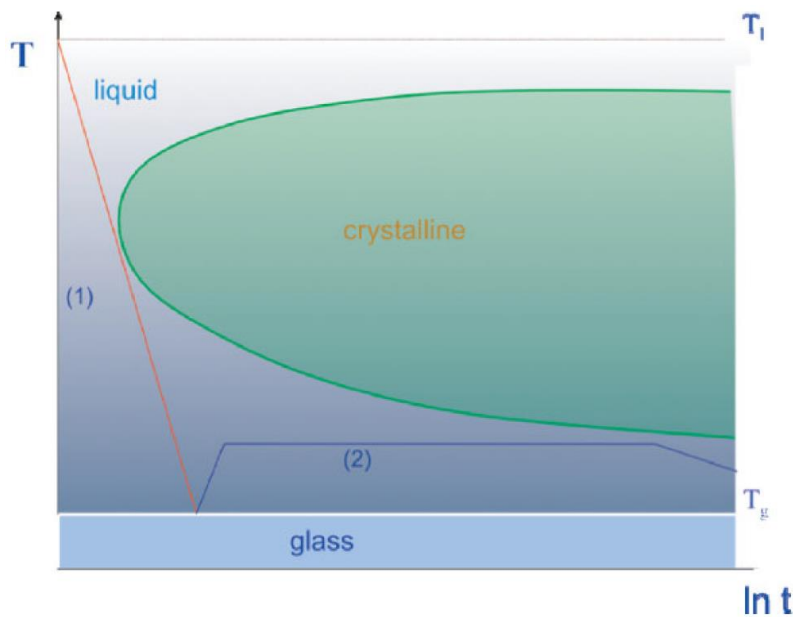


Figure 3: Schematic TTT diagram where line (1) indicates the slowest cooling rate possible to avoid crystallisation and achieve the metallic glass state, and line (2) an elevated temperature processing window above  $T_g$  where metallic glass displays excessive plastic deformation. Reproduced from [8].

These methods are well suited to the production of BMG substrates, but are of no use for forming thin film metallic glass (TFMG). The TFMGs of primary interest for these works must be quenched from the vapour state onto a substrates via the techniques detailed in the next section.

## 3.2 THIN FILMS

### 3.2.1 Deposition

TFMG coatings are readily produced via vapour deposition (VD) processes such as the physical vapour deposition (PVD) processes of pulsed laser deposition (PLD) and sputtering. These processes produce the films by condensing vaporised material onto a solid substrate under low vacuum.

#### 3.2.1.1 Pulsed Laser Deposition (PLD)

Pulsed laser deposition (PLD) produces films primarily via a thermal process under ultrahigh vacuum (UHV). The process requires a 'target' of the desired film material to be irradiated and locally vaporised by 45° inclined laser photon pulses. This results in a primarily perpendicular plasma plume of the target atoms directed toward the substrate, which on contact are deposited. Over the course of thousands of repetitions the build-up of atoms results in the film (Figure 4).

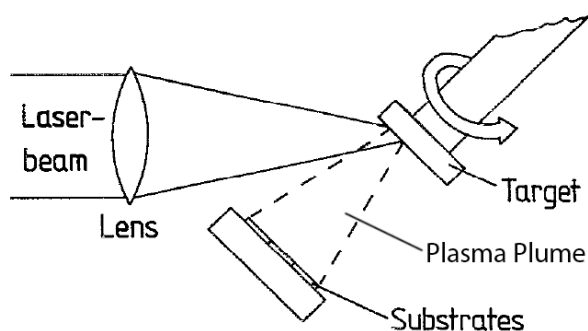


Figure 4: Schematic of a typical PLD setup showing the incoming laser beam inclined at an approximate 45° angle to the target, and the target and substrate parallel to each other. Adapted from [9].

The key advantage of PLD is it is able to deposit films of the same stoichiometric ratio as its targets [10, 11]. This is significant because it means deposited films have the same elemental composition as their target material. As the compositions of BMGs are generally carefully chosen this is practically useful as it streamlines achieving the desired TFMG compositions.

The work of Cao [12] has identified potential problems in PLD deposition of TFMGs with achieving quality surface finishes and recrystallization of amorphous targets. It appears the deposition times of the PLD allow for sufficient heat to be applied to amorphous targets to cause partial crystallisation (Figure 5), while still achieving amorphous TFMGs depositions onto the examined crystalline zirconium substrates. As PLD is a by definition a thermal deposition process preventing this heat from entering the targets could be difficult. And it remains to be examined if this excess heat could affect the substrates; ie recrystallization of amorphous BMG, polycaprolactone (PCL) scaffolds strength, thermal breakdown of the scaffold payloads, etc. Naturally this heat is a moot point when examining standalone TFMGs as these specimens are separated from their substrate after deposition.

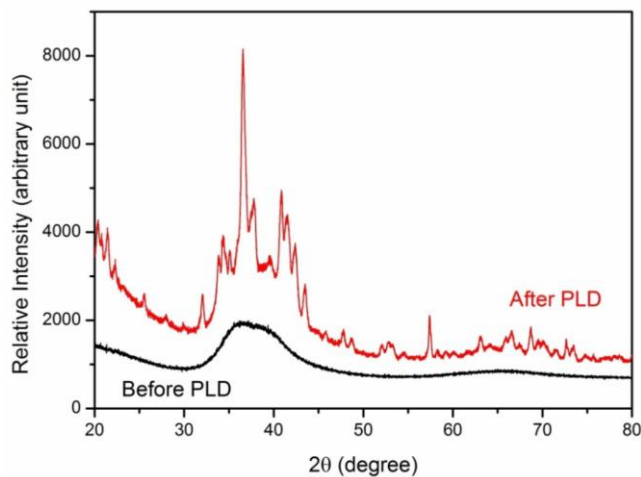


Figure 5: Amorphous target XRD scan before (black curve) and after (red curve) PLD showing the shift from characteristic amorphous structure to crystalline. Reproduced from [12].

PLD TFMG surface finish droplet defects have been observed by Krebs and Bremert [9] and later Cao [12]. It is suggested these defaults are intrinsic to the setup configuration and cannot be eliminated by refining the parameters. It is further proposed it may be possible to achieve higher quality surface finishes with setup modifications such as the addition of a mechanical velocity filter to remove slower, droplet depositing prone particles from the plasma plume. Another option is dual-beam ablation geometry which utilized two colliding laser ablation to redirect the coating to a substrate outside the direct path of both plumes preventing heavier droplet depositing prone particles from reaching the substrate. Notes both of these methodologies reduce the deposition rate and it remains to be seen if these changes are practical to implicate at UNSW.

### 3.2.1.2 Sputtering Deposition

Sputtering deposition is similar to PLD in that it coats a substrate with material transferred from a target, the essential difference being that it utilises the momentum of colliding ions, instead of lasers, to accomplish the transfer.

#### 3.2.1.2.1 Direct Current (DC) Sputtering

Direct Current (DC) sputtering applies a high-voltage to create a circuit between the target and substrate, forming a negative (cathode) and positive (anode) electrode respectively. The high-voltage field generated within the chamber ionises the low pressure inert working gas, generally Argon, causing the now positive ions to be attracted to the negative target. The charged ions collide with the target and dislodge atoms as a plasma from its surface, which are expelled in all directions. A portion of these free atoms come in contact with the substrate surface and are deposited as the coating (Figure 6).

**Commented [SG3]:** Are both the Ar and target a plasma?  
Or is it just the target atoms?  
Is the target plasma 'neutral' charge?  
Is the material not caught in the field because the momentum overcomes it?

**Commented [SG4]:** Are atoms dislodge as a plasma or are they plasma-ised in the field?

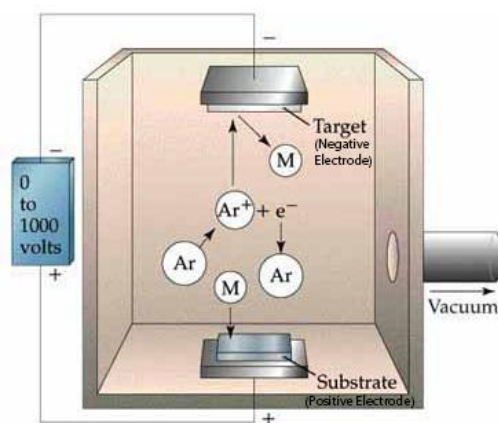


Figure 6: Schematic of a typical DC sputtering setup with an Ar working gas. The high-voltage field generates and propels  $\text{Ar}^+$  ions toward the negative target of material "M." Dislodged "M" atoms are hurled in all directions with some being deposited on the positive substrate. Adapted from [13].

The key advantage of DC sputtering when working with amorphous materials is it able to accommodate low working temperatures as the mechanical mechanism avoids adding unnecessary heat to targets and substrates. Additionally, while Ar is a convenient working gas, greater deposition efficiency can be achieved when coating with lighter or heavier elements by working with lighter or heavier inert gases, respectively. These characteristics help make it possible to deposit most BMGs via DC sputtering.

#### 3.2.1.2.2 Magnetron Sputtering

Magnetron sputtering is a variant of DC sputtering which improves ionisation efficiency by applying a magnetic field to trap the charged  $\text{Ar}^+$  ions near the target surface. This variant has proven popular in recent studies and all further mention of sputtering shall be magnetron sputtering, unless otherwise noted.

While the momentum exchange mechanism of sputtering allows for the use of amorphous targets when depositing TFMG (ie excess heat is not added to the system) it has been found the use of crystalline targets results in no appreciable difference in the quality, composition, and structure of the substrate coating [2]. Instead, as shown by Liu, et al. [2] work on the  $\text{Zr}_{55}\text{Cu}_{30}\text{Ni}_{15}\text{Al}_{10}$  system, the coating quality and production of TFMG is primarily controlled by the Ar pressure and sputtering power parameters. This has implication for practical application production runs as crystalline targets are easier, quicker and cheaper to produce than amorphous ones.

When depositing TFMGs it has been observed the deposition rate is proportional to the sputtering power, and that higher rates result in smoother film surfaces [2, 12]. Additionally, Liu, et al. [2] have found a dynamic smoothing effect occurs making it possible to produce atomically flat TFMGs with low Ar pressure and high sputtering power.

One of the core challenges with single target magnetron sputtering is it can be difficult to achieve the same composition as the target alloy when depositing multi-component TFMGs [2, 12, 14]. This can occur because of the different sputtering yield of composition target elements when subjected to ion bombardment. It is possible to remedy the situation through the use of multiple pure element targets, called combination deposition [15-17], but as shown by Liu, et al. [2] this method may not be

**Commented [SG5]:** Find more sources to back this up. Jake got closer to this conclusion, but did not quite make it.

**Commented [SG6]:** i.e. same stoichiometric ratio

**Commented [SG7]:** Can you do this to make it clear these are 'combination sputtering' references? Or do they have to go at the end of the sentence where this information will be lost?

necessary. Liu, et al. [2] found it is possible to deposit TFMGs with the same composition as their  $\text{Zr}_{55}\text{Cu}_{30}\text{Ni}_5\text{Al}_{10}$  target by refining the Ar pressure and sputtering power parameters. As this solution requires only a single target and no modifications to the sputtering set up it seems reasonable to examine it first with Mg based systems.

Thus despite sputtering having more difficulties than PLD when refining the stoichiometric ratios for deposition, it has been concluded it the superior deposition method. This is primarily because of its significant advantages; non-thermal process, lower vacuum pressures, faster deposition rates, and better surface finishes. For these reason sputtering shall be the preferred method for TFMG deposition in these works.

### 3.2.2 Thin Film Properties

Thin films have been shown to increase a BMGs bending ductility [18].

### 3.2.3 Thin Film Adhesion

The adhesion of films is readily tested via scat methods [19-22].

### 3.2.4 Ultrastable Metallic Glass (SMG)

Ultrastable glasses (USGs) are amorphous films in a low energy state produced via VD techniques and generally characterised by their high thermodynamic and kinetic stabilities, densities, elastic moduli, and always by an enhanced glass transition temperature ( $\delta T_g$ ). The  $\delta T_g$  phenomenon is their defining characteristic as it suggest the high kinetic stability because of the higher temperatures required to dislodge their atoms from the glassy configuration [23, 24]. This naturally extends to give USGs higher service temperatures, and hence higher melting temperatures relative to their traditional non-stable counterparts.

#### 3.2.4.1 SMG Production

To date the only developed USGs are of organic, molecular and polymer glasses, with very few attempts being made to produce ultrastable metallic glasses (SMGs) [1]. Part of the reason for this is it unclear if the more simple atomic structures of metallic alloys, relativity to molecular and polymer glasses, are suitable to form USGs [1]. Nevertheless the work of Yu, et al. [1] on  $\text{Zr}_{65}\text{Cu}_{27.5}\text{Al}_{7.5}$  has helped to established initial understanding of what appears to be SMGs, though it remains to be seen if the established trends extend to other metallic systems.

Production of USGs is via VD techniques onto a substrate at an elevated temperature. The initial work on USGs has shown the more complicated the deposition material's atomic structure the higher the substrate temperature ( $T_{sub}$ ) needs to be [1]. Thus while the ideal  $T_{sub}$  for a MG is  $0.7 - 0.8 T_g$ , it is  $0.75 - 0.85 T_g$  for the more complicated molecular glasses [1, 23-26]. Yu, et al. [1] goes on to note while it appears more complicated atomic structures require higher temperatures to arrange into USG configurations no definite mechanism has been identified for why USGs have ideal ranges well below their  $T_g$ , as higher temperatures would allow for more efficient rearrangement of atoms.

The molecular relaxation kinetics of glasses are the reason VD techniques are required to produce the unique properties of USGs. This is easily demonstrated with organic glass where a reduction in cooling rate by a factor of 10 typically only decreases the  $T_g$  by about 3 kelvin [4, 24]. The results of the VD techniques cannot even be replicated with extensive artificial aging or annealing times below the  $T_g$ . For example Swallen, et al. [23] found with molecular glass the ultrastable effects could not be replicated even when annealed below their  $T_g$  for 6 months, and when working with Kearns, et al. [26] went on to show the theoretical annealing time required would be at least 1000 years.

**Commented [SG8]:** Yu only used "enthalpy"  
Kearns uses both "enthalpy" and "entropy"  
Double check and make sure you did not mix either one up.

**Commented [SG9]:** The optimal range may be below  $T_g$  because surface atom can move as fast as the SCL at lower temps (still being debated). This may be why metallic glass has the lowest optimal temp range and time to from ultrastable glass (ie less energy for molecules/atoms to relax or reach ultrastable configurations). {Yu, 2013 #17}

**Commented [SG10]:** Dawson reference other papers before this, but made the conclusion. Can I site him, or should I go to his source material?  
Check the "Tg & Tf paper" as it should have first principles reference to this.

**Commented [SG11]:** Organic or molecular?

#### 3.2.4.1.1 Potential Production Issues

Investigation has found there may be issues with the  $T_{sub}$  and PVD deposition rates when producing SMGs. For example, while it has been demonstrated an elevated  $T_{sub}$  is an inherent requirement to produce USGs (see 3.2.4.1 SMG Production), Qin, et al. [16] found when working with the binary amorphous  $Zr_{65}Cu_{35}$  system raising substrates to just room temperature could cause crystallization of the films. This appears concerning as the alloy constituents of this system are in comparable amounts with the Yu, et al. [1]  $Zr_{65}Cu_{27.5}Al_{7.5}$  system. However this supports the theory that simple atomic structures metallic alloys may not be suitable to form SMGs, and it may be only more atomically complicated MGs, such as ternary systems, are suitable to form SMGs [1]. As this research will be working with ternary Mg systems, it is believed they may be sufficiently atomically complicated to form SMGs.

**Commented [SG12]:** Work on the sentence structure here as this is an important conclusion to make.

It is known from Liu, et al. [2] and Cao [12] that higher deposition rates result in smoother TFMGs, though Kearns, et al. [26] work with molecular USGs have found lower deposition rates produce more kinetically stable, lower enthalpy glasses. Interestingly when Yu, et al. [1] produced SMGs they possess both high kinetic stability and high enthalpy (see 3.2.4.2 SMG Properties and Characteristics). As Yu, et al. [1] did not examine deposition rates this means it may be possible to produce lower enthalpy SMGs with lower deposition rates, although the films may become more rough. It is simply not known if the established deposition rates of TFMGs translate to SMGs.

**Commented [SG13]:** Liu mentions surface column growth at low deposition rates, and Yu says at low rates surface molecules are more mobile and have more time for configuration sampling.

#### 3.2.4.2 SMG Properties and Characteristics

The defining characteristic of USG is an  $\delta T_g$  and accordingly high kinetic stability. They generally also are at a low-thermodynamic-energy state exhibited as a low enthalpy, have a high density, and possess a high elastic modulus.

##### 3.2.4.2.1 Differential Scanning Calorimetry (DSC), Kinetic Stability and Enthalpy

Differential scanning calorimetry (DSC) is an analytical technique that measures the heat flow of an unknown sample. This is done by raising its temperature linearly at the same rate as a reference sample with a known heat capacity. This allows phase changes to be detected in the unknown sample as more or less heat will need to be applied to it to maintain both samples at the same temperature. This can be used to detect melting, crystallising, and more suitable changes like glass transition in a sample.

With amorphous materials the output displays an exothermic 'step in the baseline' as the sample reaches its  $T_g$  because it undergoes a change in its heat capacity. Upon further heating many amorphous materials spontaneously rearrange themselves in an ordered crystalline structure. This Crystallisation temperature ( $T_x$ ) is recorded as an exothermic peak. With further heating the melting temperature ( $T_m$ ) is reached and recorded as an endothermic peak, absorbing energy.

Using DSC the kinetic stability of glass can be measured by shifts in the onset temperature ( $T_{onset}$ ), which appear as the first 'step in the baseline' in the DSC specific heat capacity ( $C_p$ ) trace; identifying the start of the  $T_g$  region. Shifts in the  $T_{onset}$  to higher temperatures identify an increase in heat capacity as the atoms need to absorb more energy to become mobile; indicating the high kinetic stability with a higher  $T_g$  [26]. The value of the  $T_g$  is generally taken as the maxima of the derivative of trace with respect to temperature.

A specific enthalpy ( $h$ ) curve from the DSC trace can be obtained by integrating the original  $C_p$  trace, with respect to temperature. Using this curve the fictive temperature ( $T_f$ ) can be used to establish the enthalpy of the film by measuring where the film's enthalpy line intersects the extrapolated SCL enthalpy



line of the bulk material (Figure 7) [26]. A non-stable glass' enthalpy appears at  $T_f = T_g$  on the trace, whereas a stable glass' is expected to have a lower  $T_f$  and lower enthalpy at  $T_f < T_g$ .

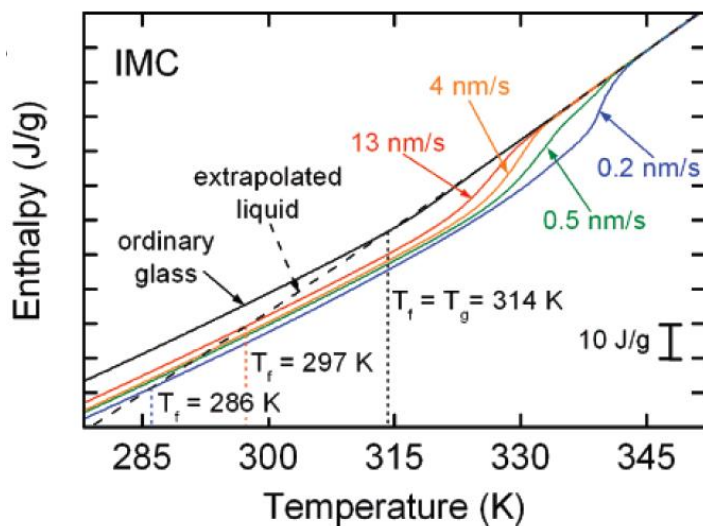


Figure 7: An integrated DSC trace for the molecular IMC glass system displaying the various values of  $T_f$  obtained when varying the deposition rate (the coloured line). Note all deposited glasses have a reduced  $T_f$  indicating a reduction in enthalpy compared to ordinary glass. Reproduced from [26].

However the work Yu, et al. [1] and Guo, et al. [27] on SMGs and polymer USGs respectively have shown an  $\delta T_g$  with its high kinetic stability can be coupled with high enthalpy. When this happens the enthalpy traces of USGs are greater than non-stable glass and intersect higher on the SCL line with a  $T_f > T_g$ . This contradiction with Kearns, et al. [26] demonstrates that  $T_{onset}$  and  $T_f$  are not coupled together and act independently in USG systems.

#### 3.2.4.2.2 The Theoretical Entropy Limit of Glasses and the Kauzmann Temperature $T_k$

Normally a glass is formed when its SCL solidifies on reaching its  $T_g$ . However if the SCL can be lower to the entropy of its crystalline state it will achieve the theoretical lowest thermodynamic-energy state possible and its 'ideal'  $T_g$ , known as the Kauzmann temperature ( $T_k$ ), (Figure 8) [23, 26]. This makes  $T_k$  a useful limit to evaluate the effectiveness of the improvements in thermodynamic stability of USGs.

**Commented [SG14]:** Have some other references around this point. Should have a look at them.

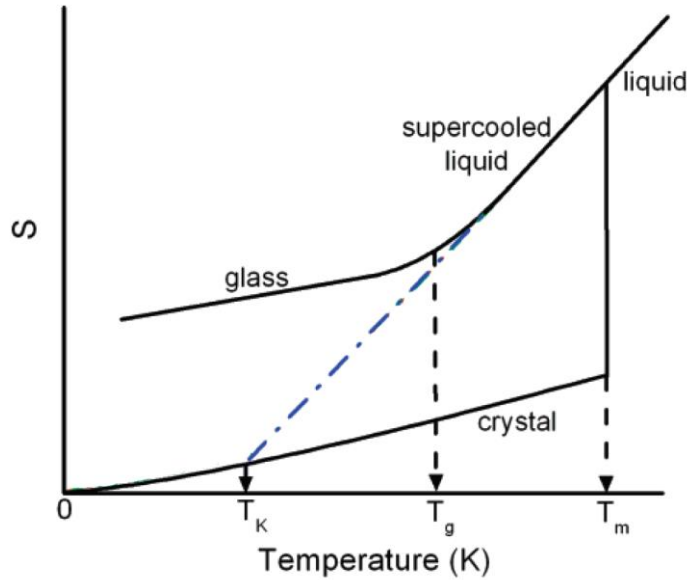


Figure 8: Schematic of solidification/liquid glass temperature vs entropy in a typical glass forming system. The Kauzmann temperature ( $T_k$ ) represents the glass transition temperature ( $T_g$ ) of an ideal glass. The blue line is the extrapolated SCL line and the ideal path. Modified from [26].

Using Swallen, et al. [23] and Kearns, et al. [26] equation for proportion along the energy landscape ( $\theta_k$ ) following the extrapolation SCL blue line, the reduction in the glass' entropy compared to its non-stable variant can be calculated.

$$\theta_k = \frac{T_g - T_f}{T_g - T_k} \quad (3.1)$$

From equation (3.1) it can be seen a non-stable glass with  $T_f = T_g$  will result in  $\theta_k = 0$ , signifying the glass has not moved down the energy landscape, while an ideal glass with  $T_f = T_k$  will result in  $\theta_k = 1$ , signifying the glass has reached the bottom of the energy landscape [23, 26]. Therefore for real USGs with reduced entropy the  $\theta_k$  will fall between 0 and 1, while the SMGs of Yu, et al. [1] which were found to have increased entropy would yield a  $\theta_k$  of less than 0, indicating they have moving up the energy landscape. For example, a  $\theta_k = -0.25$  would indicate the USG's entropy is 125% greater than the 'ideal' glass ('ideal' glass has  $T_g = T_k$ ).

#### 3.2.4.2.3 Glass Fragility $m$

The fragility ( $m$ ) of a glass is a measure of its deviation from ideal Arrhenius behaviour, defined by a function of variation in the glass' viscosity ( $\eta$ ) with respect to temperature normalized by  $T_g$ .

**Commented [SG15]:** When values are negative formula indicates an increase in entropy.

Maybe try to rewrite to reflect all changes in entropy with a meaningful output (instead of just improvements).

$$m \equiv \left. \frac{\partial \log_{10}(\eta)}{\partial \left(\frac{T_g}{T}\right)} \right|_{T=T_g} \quad (3.2)$$

The more a glass varies from this ideal Arrhenius behaviour the more ‘fragile’ it is, and higher its  $m$  value. Highly fragile glasses vary significantly from the ideal Arrhenius behaviour and are termed ‘weak,’ generally experience significant deviations in heat capacity with temperature [28]. In contrast low fragility, or ‘strong’ glasses, have little variation from Arrhenius behaviour and usually experience little change in heat capacity with temperature. Whether a glass is strong or weak typically depends on the atomic structure, with MGs generally characterised as ‘strong’, polymers as ‘weak,’ and molecular glasses somewhere between, see Figure 9.

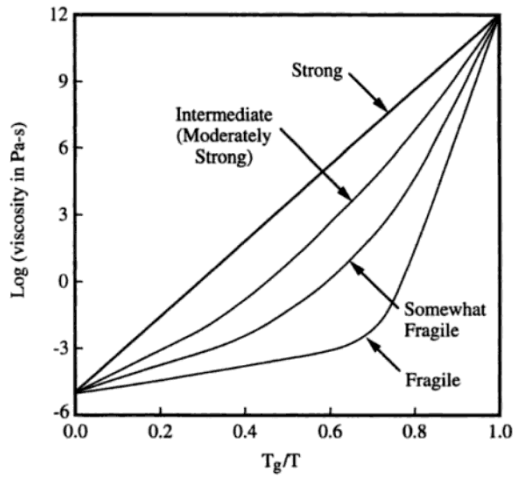


Figure 9: Schematic of fragility for strong and weak glasses over the liquid range of viscosities. Note the ‘ideal’ strong liquid display a constant exponential slope over the full temperature range, while weaker liquids’ slopes change. Reproduced from [28].

Yu, et al. [1] found  $m$  of metallic, molecular, and polymer USGs correlate with  $\delta T_g/T_g$ , which is surprising given the notable difference in their atomic structures, bonding, and deposition rates (Figure 10). From these initial findings it appears greater improvements in  $\delta T_g$  in relation to the standard  $T_g$  correlates with more fragile glasses (i.e. a high  $m$  values supports a high  $\delta T_g$ ). This suggests the  $\delta T_g$  improvements for SMGs may have a modest limit.

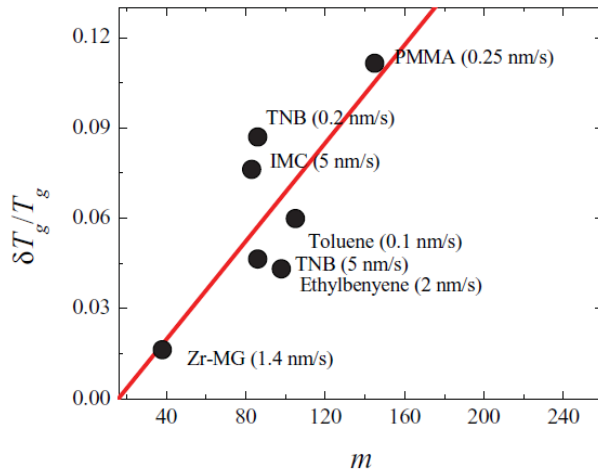


Figure 10: Schematic of the relationship between glass fragility ( $m$ ) and the enhanced glass transition on glass transition ( $\delta T_g / T_g$ ) for a selection of metallic, molecular, and polymer USGs. Reproduced from [1].

#### 3.2.4.2.4 Indentation Modulus $M$

SMG has larger 'Indentation Modulus  $M$ ' than MG.

$$M \equiv \frac{E}{(1 - \nu^2)} \quad (3.3)$$

(around a 5 - 10% improvement from MG to SMG)

XRD cannot distinguish MG from SMGs.

(From molecular glasses (ie traditional glasses) would expect SMGs to show extra-low angle peaks)

May indicate a hidden polyamorphous or layer-like super-structures.

May indicate the corresponding states of packing are not drastically different.

It has been established that TFMGs display different characteristics from BMGs. Coating of TFMGs directly onto BMGs can affect the BMGs characteristics. From "Bendable Metallic Glasses???"

### **3.3 BIOMEDICAL**

Need to have section with the typical ranges of human bone hardness and E (most studies use these two parameters but do not include a human bone hardness for comparison).

#### **3.3.1 Bioreabsorption / Corrosion**

As Witte [29] has shown in his review magnesium was showing promise as a bioreabsorbable material in the early 1900s before the trend switch to bioinert materials like titanium.

Challenges with bioreabsorbable metals, need to;

- reduce the level of ion toxicity
- reduce the amount of hydrogen gas
- control the loss of mechanical strength over time.

High Zn content in MgZnCa decreases hydrogen evolution and promotes passive corrosion.

#### **3.3.2 Anti-biotic Scaffolds**

## 4 REFERENCES

- [1] H.-B. Yu, Y. Luo, and K. Samwer, "Ultrastable Metallic Glass," *Advanced Materials*, vol. 25, pp. 5904-5908, 2013.
- [2] Y. H. Liu, T. Fujita, A. Hirata, S. Li, H. W. Liu, W. Zhang, *et al.*, "Deposition of multicomponent metallic glass films by single-target magnetron sputtering," *Intermetallics*, vol. 21, pp. 105-114, 2// 2012.
- [3] A. L. Greer, Y. Q. Cheng, and E. Ma, "Shear bands in metallic glasses," *Materials Science and Engineering: R: Reports*, vol. 74, pp. 71-132, 4// 2013.
- [4] M. Ediger, C. Angell, and S. R. Nagel, "Supercooled liquids and glasses," *The journal of physical chemistry*, vol. 100, pp. 13200-13212, 1996.
- [5] W. Klement, R. Willens, and P. Duwez, "Non-crystalline structure in solidified gold-silicon alloys," 1960.
- [6] A. Inoue, "Stabilization of metallic supercooled liquid and bulk amorphous alloys," *Acta Materialia*, vol. 48, pp. 279-306, 1/1/ 2000.
- [7] M. M. Trexler and N. N. Thadhani, "Mechanical properties of bulk metallic glasses," *Progress in Materials Science*, vol. 55, pp. 759-839, 11// 2010.
- [8] J. Schroers, "Processing of Bulk Metallic Glass," *Advanced Materials*, vol. 22, pp. 1566-1597, 2010.
- [9] H. U. Krebs and O. Bremert, "Pulsed laser deposition of thin metallic alloys," *Applied Physics Letters*, vol. 62, pp. 2341-2343, 1993.
- [10] D. Dijkkamp, T. Venkatesan, X. Wu, S. Shaheen, N. Jisrawi, Y. Min-Lee, *et al.*, "Preparation of Y-Ba-Cu oxide superconductor thin films using pulsed laser evaporation from high Tc bulk material," *Applied Physics Letters*, vol. 51, pp. 619-621, 1987.
- [11] J. Heitz, X. Wang, P. Schwab, D. Bäuerle, and L. Schultz, "KrF laser-induced ablation and patterning of Y-Ba-Cu-O films," *Journal of Applied Physics*, vol. 68, pp. 2512-2514, 1990.
- [12] J. D. Cao, "Processing and properties of biocompatible metallic glasses," M. Ferry and K. Laws, Eds., ed: Thesis (Ph.D) - University of New South Wales - Australia, 2013.
- [13] T. E. Brown, T. L. Brown, H. E. H. LeMay, B. E. Bursten, C. Murphy, and P. Woodward, *Chemistry: The Central Science*: Pearson Education, 2014.
- [14] K. Kondoh, K. Kawabata, T. Serikawa, and H. Kimura, "Structural Characteristics and Crystallization of Metallic Glass Sputtered Films by Using Zr System Target," *Advances in Materials Science and Engineering*, vol. 2008, 2008.
- [15] Y. P. Deng, Y. F. Guan, J. D. Fowlkes, S. Q. Wen, F. X. Liu, G. M. Pharr, *et al.*, "A combinatorial thin film sputtering approach for synthesizing and characterizing ternary ZrCuAl metallic glasses," *Intermetallics*, vol. 15, pp. 1208-1216, 9// 2007.
- [16] J. Qin, X. Yong, Z. Xin-Yu, L. Gong, L. Li-Xin, X. Zhe, *et al.*, "Zr-Cu amorphous films prepared by magnetron co-sputtering deposition of pure Zr and Cu," *Chinese Physics Letters*, vol. 26, p. 086109, 2009.
- [17] M. Apreutesei, P. Steyer, L. Joly-Pottuz, A. Billard, J. Qiao, S. Cardinal, *et al.*, "Microstructural, thermal and mechanical behavior of co-sputtered binary Zr-Cu thin film metallic glasses," *Thin Solid Films*, vol. 561, pp. 53-59, 6/30/ 2014.
- [18] J. P. Chu, J. E. Greene, J. S. C. Jang, J. C. Huang, Y.-L. Shen, P. K. Liaw, *et al.*, "Bendable bulk metallic glass: Effects of a thin, adhesive, strong, and ductile coating," *Acta Materialia*, vol. 60, pp. 3226-3238, 4// 2012.
- [19] S. J. Bull and A. M. Jones, "Multilayer coatings for improved performance," *Surface and Coatings Technology*, vol. 78, pp. 173-184, 1// 1996.
- [20] P. J. Burnett and D. S. Rickerby, "The relationship between hardness and scratch adhesion," *Thin Solid Films*, vol. 154, pp. 403-416, 11/12/ 1987.

- [21] P. J. Burnett and D. S. Rickerby, "The scratch adhesion test: An elastic-plastic indentation analysis," *Thin Solid Films*, vol. 157, pp. 233-254, 2/29/ 1988.
- [22] C. T. Pan, T. T. Wu, C. F. Liu, C. Y. Su, W. J. Wang, and J. C. Huang, "Study of scratching Mg-based BMG using nanoindenter with Berkovich probe," *Materials Science and Engineering: A*, vol. 527, pp. 2342-2349, 4/15/ 2010.
- [23] S. F. Swallen, K. L. Kearns, M. K. Mapes, Y. S. Kim, R. J. McMahon, M. D. Ediger, *et al.*, "Organic glasses with exceptional thermodynamic and kinetic stability," *Science*, vol. 315, pp. 353-356, 2007.
- [24] K. Dawson, L. Zhu, L. A. Kopff, R. J. McMahon, L. Yu, and M. Ediger, "Highly stable vapor-deposited glasses of four tris-naphthylbenzene isomers," *The Journal of Physical Chemistry Letters*, vol. 2, pp. 2683-2687, 2011.
- [25] K. J. Dawson, L. Zhu, L. Yu, and M. Ediger, "Anisotropic structure and transformation kinetics of vapor-deposited indomethacin glasses," *The Journal of Physical Chemistry B*, vol. 115, pp. 455-463, 2010.
- [26] K. L. Kearns, S. F. Swallen, M. Ediger, T. Wu, Y. Sun, and L. Yu, "Hiking down the energy landscape: Progress toward the Kauzmann temperature via vapor deposition," *The Journal of Physical Chemistry B*, vol. 112, pp. 4934-4942, 2008.
- [27] Y. Guo, A. Morozov, D. Schneider, J. W. Chung, C. Zhang, M. Waldmann, *et al.*, "Ultrastable nanostructured polymer glasses," *Nature materials*, vol. 11, pp. 337-343, 2012.
- [28] J. E. Shelby, *Introduction to Glass Science and Technology*: Royal Society of Chemistry, 2005.
- [29] F. Witte, "The history of biodegradable magnesium implants: A review," *Acta Biomaterialia*, vol. 6, pp. 1680-1692, 5// 2010.

## 5 APPENDICES

---

### 5.1 GLOSSARY

BMG	–	Bulk Metallic Glass
$C_p$	–	Specific Heat Capacity ( $J / gK$ )
CVD	–	Chemical Vapour Deposition
DC	–	Direct Current ( $I$ )
DSC	–	Differential Scanning Calorimetry
$E$	–	Young's Modulus ( $GPa$ )
GFA	–	Glass Forming Ability
$H$	–	Enthalpy ( $J$ )
$h$	–	Specific Enthalpy ( $J / g$ )
$m$	–	Fragility
MG	–	Metallic Glass
PCL	–	Polycaprolactone
PLD	–	Pulse Laser Deposition
PVD	–	Physical Vapour Deposition
$R_c$	–	Critical Cooling Rate ( $K / s$ )
SCL	–	Super Cooled Liquid
SMG	–	Ultrastable Metallic Glass
$T_f$	–	Fictive Temperature ( $K$ )
TFMG	–	Thin Film Metallic Glass
$T_g$	–	Glass Transition Temperature ( $K$ )
$T_g/T_m$	–	Reduced Glass Transition Temperature ( $K$ )
$T_k$	–	Kauzmann Temperature ( $K$ )
$T_m$	–	Melting Temperature ( $K$ )
$T_{onset}$	–	Onset Temperature ( $K$ )
TPF	–	Thermoplastic Forming
$T_{sub}$	–	Substrate Temperature ( $K$ )
$t_{max}$	–	Maximum Sample Thickness ( $mm$ )



$T_x$	–	Crystallisation Temperature ( $K$ )
UHV	–	Ultrahigh Vacuum
UNSW	–	University of New South Wales
USG	–	Ultrastable Glass
$V$	–	Volume ( $m^3$ )
$v$	–	Specific Volume ( $m^3 / kg$ )
VD	–	Vapour Deposition
$\delta T_g$	–	Enhanced Glass Transition Temperature ( $K$ )
$\eta$	–	Viscosity ( $Pa\ s$ )
$\theta_k$	–	Proportion along the Energy Landscape